ELSEVIER

Earth and Planetary Science Letters 204 (2002) 151–165

EPSL

www.elsevier.com/locate/epsl

Oxygen isotope evidence for progressive uplift of the Cascade Range, Oregon

Matthew J. Kohn [a,*], Jennifer L. Miselis [a,1], Theodore J. Fremd [b]

[a] *Department of Geological Sciences, University of South Carolina, Columbia, SC 29208, USA*
[b] *John Day Fossil Beds National Monument, Kimberly, OR 97848, USA*

Received 13 May 2002; received in revised form 4 September 2002; accepted 4 September 2002

Abstract

Oxygen isotope compositions of fossil equid teeth in the Cascade rainshadow reveal a ~5‰ decrease in mean $\delta^{18}O$ since 27 Ma. Isotopic changes are inconsistent with expected effects from global climate change because: (a) the expected isotopic shift to tooth $\delta^{18}O$ values due to global climate change (~1‰) is much smaller than the observed shift, (b) predicted and observed isotopic trends are opposite for Oligocene vs. Miocene samples, and (c) average compositions and ranges in compositions remained unchanged for samples from before and after major global cooling in the mid-Miocene. Accounting for a decrease in relative humidity of at least 15%, we infer a topographically driven secular shift in the $\delta^{18}O$ value of rainwater of 6–8‰ since the late Oligocene, which is approximately equivalent to the modern-day difference in $\delta^{18}O$ values of precipitation and surface waters across the central Cascades. Rise of the central Cascades apparently occurred monotonically over the last 27 Ma, with a hiatus between ~15.4 and 7.2 Ma, possibly related to eruption of the Columbia River Basalts. Progressive volcanic accumulation over tens of millions of years best explains the data, rather than a short-lived uplift event. Paleoseasonality, as inferred from isotope zoning and intertooth variability, decreased dramatically from 7–9‰ at 15.4–7 Ma to ~3‰ at 3 Ma, then increased to 6–8‰ today. The cause of the decrease in seasonality at 3 Ma may reflect either brief warming during the mid-Pliocene within the context of global tectonic reorganization, or consumption by equids of water from an isotopically buffered Lake Idaho.

Keywords: Oregon; Cascades; paleoclimatology; teeth; enamel; oxygen; stable isotopes

1. Topographic uplift and the Cascade Range

Topographic uplift of mountain ranges and plateaus strongly affects climate [1], and is intimately tied to the physical/chemical state of the crust and upper mantle [2], including variations in crustal and lithospheric thickness, thermal structure and/or bulk chemical properties. Because of their climatic impact, surface uplift and lithospheric properties may be monitored accurately by using

* Corresponding author. Tel.: +1-803-777-5565; Fax: +1-803-777-6610.
E-mail addresses: mjk@geol.sc.edu (M.J. Kohn), jmiselis@vims.edu (J.L. Miselis), ted_fremd@nps.gov (T.J. Fremd).

[1] Present address: School of Marine Science, Virginia Institute of Marine Sciences, Gloucester Point, VA 23062, USA.

0012-821X/02/$ – see front matter
PII: S0012-821X(02)00961-5

the $\delta^{18}O$ values of rainwater. In general, higher mountains cause greater rainout that decreases the ^{18}O of surface waters in the rainshadow, so that a history of rainwater $\delta^{18}O$ values in a rainshadow should reflect the changing altitude of the mountains. In this study, we measured $\delta^{18}O$ values of fossil teeth in the rainshadow of the central Cascades in Oregon as a proxy for paleo-rainwater $\delta^{18}O$. These data show a gradual ^{18}O depletion over the last 27 Myr, which we believe indicates progressive uplift of the range, and a progressive change to the bulk properties of the lithosphere.

The Cascade Range is a continental volcanic arc that results from the subduction of the Juan de Fuca plate beneath North America (Fig. 1). The Cascades had and continue to have an impressive impact on regional climate. Coastal Oregon has high rainfall (150–200 cm/yr) and high relative humidity (80%), whereas central Oregon has low rainfall (25 cm/yr) and low humidity

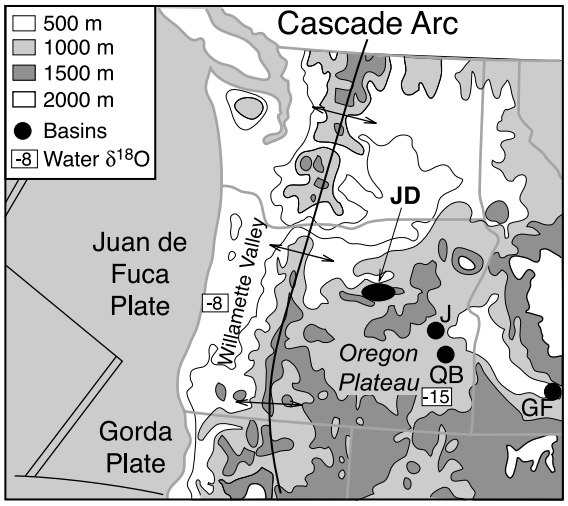

Fig. 1. Generalized topographic map of northwestern US, showing basic tectonic framework, trend of Cascade arc, and location of basins investigated in this study. JD = John Day Basin (John Day, Mascall, and Rattlesnake Formations; modern cow); J = Juntura; QB = Quartz Basin; GF = Glenns Ferry. Although most basins are within the elevated Oregon plateau, they represent topographic lows not resolvable at this scale. All study areas are affected climatically by rainout over the Cascade range. Negative numbers refer to regional streamwater and/or springwater $\delta^{18}O$ values (V-SMOW; [4–6]), and are not significantly different among sites in interior Oregon.

(50%) [3]. Because rainout depletes subsequent rainfall in ^{18}O, rainwater and surface water $\delta^{18}O$ values for the Oregon interior, east of the Cascades, are substantially ^{18}O-depleted ($\sim$7‰) compared to coastal Oregon and the Willamette Valley [4–6]. In the past, when the Cascades were lower, rainout must have been less effective and interior rainfall amounts and $\delta^{18}O$ values should have been higher. Indeed, paleoflora and paleosols in central Oregon attest to paratropical and temperate forests prior to $\sim$34 Ma, intermixed grassy woodlands and wooded grasslands until at least 15 Ma, grasslands by $\sim$7.2 Ma, and near-modern conditions by $\sim$4 Ma [7,8]. Based on regional meteorological data linked to the National Climatic Data Center's website [9], comparable modern-day floral assemblages in the conterminous United States exist at mean annual relative humidities of $\sim$75% (paratropical forests), $\sim$70% (woodlands), 60–70% (grasslands), and 50–55% (modern), suggesting that a quasi-continuous decrease in humidity occurred in central Oregon since the late Eocene. This drying could reflect Cascade uplift and rainshadows [7], but could alternatively be related to global climate change. Consequently, an independent measure of the rainshadow, such as the $\delta^{18}O$ values of paleo-rainwater in the lee of the range, is required to evaluate topographic evolution through time. Oxygen isotope compositions of tooth phosphate and rainwater strongly correlate, so we measured $\delta^{18}O$ values of fossil teeth from east of the Cascades as a proxy for the $\delta^{18}O$ of paleo-rainwater in the rainshadow of the rising Cascades.

Because tectonism and climate are linked, it is important to relate any paleo-rainwater trends to arc activity. Three major periods of Cenozoic magmatism have been inferred in western Oregon, as summarized by Hammond [10]. The western Cascades (immediately adjacent to the Willamette valley; Fig. 1) first formed at $\sim$40–45 Ma, and were active semi-continuously until $\sim$8 Ma, but had mostly formed by $\sim$18 Ma. Subsequent mid-Miocene magmatism was strongly subordinate to the Columbia River flood basalts, which erupted mainly between 17 and 14 Ma. Voluminous eastern Cascade volcanism began at $\sim$7 Ma and continues today. Extension at $\sim$5.4 Ma created a

graben in the eastern part of the range [11], which has largely been filled with the modern-day, eastern Cascade volcanoes and flows. The effects of each of these events on topography, if any, are unknown. Different models of Cascade topography include progressive uplift since the Eocene [10], pulsed uplift during the mid-Miocene and early Pliocene [12], and rapid post-Miocene uplift [13]. In short, interpretations run the gamut of tectonically continuous to catastrophic processes.

2. Oxygen isotopes of teeth

Oxygen isotope compositions of herbivore teeth principally depend on two factors: local water composition and humidity. Herbivore phosphate and rainwater $\delta^{18}O$ correlate strongly because large herbivores obtain the majority of their intake oxygen from drinking water (surface water from lakes and streams, springs, etc.) and from plants, whose composition is directly linked to surface water. The relation between phosphate and local water $\delta^{18}O$ is not 1:1 because atmospheric O_2 is consumed, and its isotope composition is geographically invariant. Empirical studies and theoretical models suggest a dependence of phosphate vs. local water $\delta^{18}O$ of $\sim$0.8–0.9‰ (PO_4)/1‰ (Local water). We assume that drinking water and water from plants are sourced from local precipitation, and for predictions assume an intermediate slope of 0.85‰/1‰. Phosphate $\delta^{18}O$ and humidity correlate negatively because $\delta^{18}O$ values of surface waters and plants both increase in dry settings [14]. The dependence of herbivore $\delta^{18}O$ and humidity is not well characterized, but empirical and theoretical studies suggest a slope of $\sim$0.1–0.2‰/% [14,15]. The weaker dependence assumes that humidity effects result solely from plant (food) response to humidity, whereas the stronger dependence is found in natural studies, and likely reflects some evaporative enrichment of surface waters in drier settings. Based on changes in paleoflora and paleosols, humidity must have decreased in central Oregon over the time period investigated, presumably affecting both plants and surface water, and so this secondary isotope effect must also be considered.

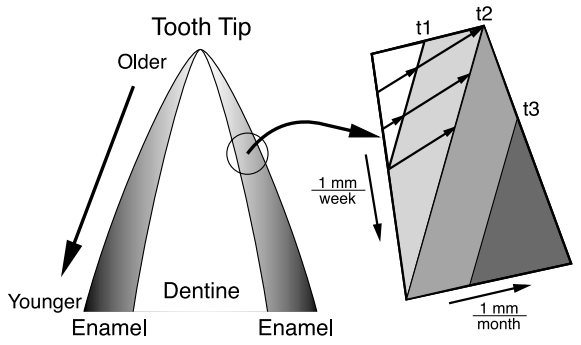

Fig. 2. Schematic of how equid enamel grows. Enamel first nucleates at the dentine–enamel junction at the crown of a tooth, and grows downward and outward through time. Studies of modern large herbivores [16–18] indicate an enamel growth rate of $\sim$1 mm/week from the occlusal surface to cervical margin. Growth bands are inclined by $\sim$15° to the dentine–enamel interface, implying that outward growth rates are $\sim$1 mm/month. All samples analyzed had enamel less than 1 mm thick, implying that sampling methods averaged compositions on a time scale less than $\sim$1.5 months.

For predictions, the full range of dependencies is considered. High-elevation low $\delta^{18}O$ runoff does not significantly bias modern-day water compositions in central Oregon [4–6]. If it did in the past, then the observed tooth isotopic trend would be underestimated.

Teeth in large herbivores require a few months to over a year to form depending on length. For enamel, a mineralizing front forms at the crown of the tooth and sweeps towards the root, producing a thin shell at a rate of $\sim$1 mm per 5–15 days ([16–18], this study; Fig. 2). Because climate and environmental $\delta^{18}O$ in most areas vary seasonally, teeth are isotopically zoned. However, teeth do not all form simultaneously, and so different teeth record different portions of the yearly seasonality. By analyzing several teeth from one locality, the true range of compositions and total climate seasonality can be identified ([17,18]; Fig. 3). Quasi-sinusoidal isotope variations are expected because of alternating high $\delta^{18}O$ summer/dry and low $\delta^{18}O$ winter/wet seasons.

3. Sampling protocol

Fossil teeth were analyzed from collections

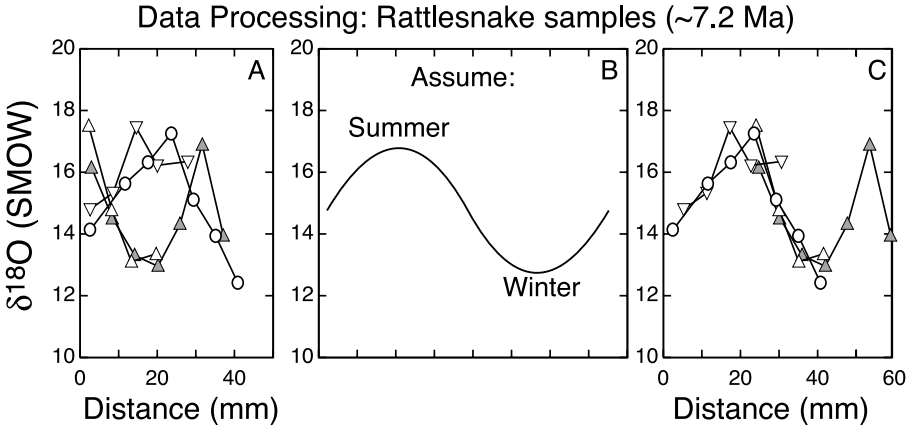

Fig. 3. Example from selected Rattlesnake Formation teeth of how data are reconciled with seasonal isotope variations. (A) Different teeth initiate formation during different seasons, so plots of composition vs. distance along tooth will show different patterns. (B) In general, isotope seasonality is predicted to behave quasi-sinusoidally, with a high $\delta^{18}O$ summer/dry season, and a low $\delta^{18}O$ winter/wet season. (C) Temporal shifting of individual tooth data sets reconciles data with a seasonal model, and reveals total seasonal isotope signal.

housed at the University of Oregon, John Day Fossil Beds National Monument, and Hagerman Fossil Beds National Monument, focusing on equid enamel to minimize any species-dependent differences in $\delta^{18}O$; modern equid and bovid teeth from near Juntura and John Day were also analyzed to provide a modern signal (Table 1). Analysis of members of sympatric orders (e.g. gomphothere, camelid, dromomerycid, oreodont, etc.) could potentially provide additional independent information on humidity changes and/or ecosystem heterogeneity, but such analysis was beyond the scope of the current project. Enamel was selected because of all biogenic tissues, it is least susceptible to diagenetic recrystallization [19], which presumably could affect isotopic compositions. PO_4 was chosen for analysis because of all oxygen-bearing components in biological apatites, it is least susceptible to isotopic alteration (e.g. [20]; see also summary of [21]). A 2–5 mm wide strip of enamel was cut lengthwise from each tooth and sectioned every 1–2 mm along the length. Although the mineralizing front may sweep along 1 mm within only ~1 week, the rate of outward enamel growth is much slower (Fig. 2). Sampling the entire thickness of enamel, as we have done, likely integrates less than 1 to perhaps 1.5 months' time [21], as the enamel is no more than 1 mm thick. This averaging is not a serious problem because organisms cannot respond instantaneously to a change in the environment. The oxygen flux per day through a large herbivore is ordinarily a small percentage of its total oxygen pool, so that residence times for oxygen are substantial, typically several weeks. Such residence times imply that compositional extremes within the environment will be smoothed, and a time lag will develop between the isotope composition that a species would have if it were instantaneously equilibrated with its environment and the actual isotope composition of the species. The degree to which the environmental signal is averaged depends on specific oxygen flux rates and the nature of the environmental signal, but for a sinusoidal variation in environmental composition and a constant residence time τ, the damping factor D and time lag Δt will be [22]:

$$D = \frac{1}{\left[\frac{2\pi\tau}{365} + 1\right]^{1/2}} \quad (1)$$

$$\Delta t = \frac{365}{2\pi}\tan^{-1}\left[\frac{2\pi\tau}{365}\right] \quad (2)$$

where τ (in days) is the total oxygen pool divided by the daily flux. Typically, animals turn over ~5–10% of their oxygen pool per day via intake

of food, water, and O_2, and loss of wastes and thermoregulatory water, leading to $\tau \sim 10$–20 days. That is, any compositional analysis, no matter how small, must average environmental isotope variations that are shorter than a few weeks because of inherent reservoir effects within the animal. Eqs. 1 and 2 show that the isotope composition of an animal is not a perfect measure of environmental seasonality, so that isotope zoning in a tooth instead reflects about 85–90% of the total seasonal signal, and lags environmental seasonality by about 2–3 weeks.

Any adhering dentine was removed from samples using a small hand-held drill. Longitudinal sections were analyzed every third sample (i.e. approximately every 5 mm) using the technique of O'Neil et al. [23] as modified by Dettman et al. [24]. Samples were dissolved in HF, the resulting CaF_2 was discarded, and Ag_3PO_4 was instantaneously precipitated by buffering the solution with NH_4OH and adding excess $AgNO_3$. The Ag_3PO_4 was combusted with graphite in silica tubes at 1200°C, and the resulting CO_2 was analyzed for $\delta^{18}O$. Sample sizes were 5–10 mg, reproducibility was $\sim \pm 0.3$‰ ($\pm 1\sigma$), and the average composition for NBS-120c was 22.4‰ (V-SMOW, Table 1). Recently, it has been shown that measured differences in isotope composition for different materials as determined using the O'Neil technique are smaller than those determined using fluorination or pyrolysis [25]. Because fluorination and pyrolysis both yield nearly 100% of oxygen, and the O'Neil method yields only 25%, the scale compression is viewed as an analytical artifact that must be corrected for accuracy. Corrections to our raw data were made based on compositions measured for NBS-120c (22.6‰, [25]) and interlaboratory comparisons of igneous apatites (UMS-1 and SP3). These corrections are negligible for samples with compositions of ~ 20‰ (e.g. 22.4 vs. 22.6‰ for NBS-120c), and ~ -1.5‰ for samples with compositions of ~ 10‰. The correction increases our inferred total isotopic shift by ~ 1‰, but does not significantly affect our main conclusions.

Six stratigraphic units in central/eastern Oregon and western Idaho were sampled: Turtle Cove member of the John Day Formation (~ 27 Ma; six teeth), Mascall and Quartz Basin Formations (both ~ 15.4 Ma; 13 teeth), Juntura Formation (~ 11 Ma; five teeth), Rattlesnake Formation (~ 7.2 Ma; eight teeth), and Glenns Ferry Formation (~ 3.2 Ma; two teeth). All ages are based on precise (± 0.1 Ma) $^{40}Ar/^{39}Ar$ single-crystal analyses of interbedded tuffs [26,27] excepting the Juntura and Quartz Basin Formations, which are constrained by less precise ages (± 0.4–1 Ma) and by tuffs elsewhere that bracket biostratigraphically useful assemblages. The John Day samples are of *Miohippus* sp., the Mascall and Quartz Basin samples are of *Merychippus* sp., and the Juntura, Rattlesnake and Glenns Ferry samples are of *Hipparion*, *Neohipparion* and *Pliohippus* sp. These genera separate into the families Anchitheriinae (*Miohippus* and *Merychippus*) and Equinae (*Hipparion*, *Neohipparion*, and *Pliohippus*), so taxon-dependent compositional differences would likely be greatest between the Mascall/Quartz basin and Juntura samples. This point is discussed in more detail in Section 4. Climatically, the John Day samples are from the late-Oligocene thermal minimum, the Mascall samples are from the mid-Miocene climatic optimum and clearly predate the global mid-Miocene shift to cooler conditions [28], and within chronologic uncertainty the Glenns Ferry samples coincide with the mid-Pliocene thermal optimum. The modern-day samples include one horse tooth and several cattle teeth. Comparison of the global data set for *Bos* and *Equus* indicates that their compositions are nearly identical [21], so they may be used interchangeably for modern-day comparisons. The modern horse tooth was incompletely mineralized at its base, so the compositions from the base of the tooth are probably not representative. The modern samples also include M1 teeth, which could have an anomalously high $\delta^{18}O$ composition because of milk consumption [29]. However, the magnitude of this effect is not well known, and two studies of wild animals have suggested no 'milk effect' [17,30]. Discarding the M1 analyses would change interpretation of the modern-day isotope signal by ~ 1‰, which does affect interpretations of the most recent isotopic change, but does not significantly affect our main conclusions.

Table 1
Oxygen isotope compositions of fossil teeth from central Oregon and western Idaho, USA

Sample[a]	Distance[b]	$\delta^{18}O$	Sample[a]	Distance[b]	$\delta^{18}O$	Sample[a]	Distance[b]	$\delta^{18}O$
John Day Formation: 27 Myr ago								
F17188/b	21.5	14.80	5795-3/a	5	16.38			
F17188/e	16	14.10	5795-3/c	1	17.98			
F17188/h	10	15.27	5795-4/b	9	17.23			
F17188/k	4	16.14	5795-4/d	4	16.72			
5795-1/c	8.75	17.80	5795-4/f	0.75	16.33			
5795-2/a	3.75	18.37	7280/b	3.5	17.07			
5795-2/b	19.92	18.17	7280/c	1.25	14.73			
Mascall Formation: 15.4 Myr ago								
2026/e	23.5	14.96	2018/b	28.5	14.48	1999/b	24.5	14.97
2026/h	17	17.35	2018/e	22.25	13.08	1999/e	19	13.48
2026/k	11	17.72	2018/h	16.5	13.44	1999/h	13	15.05
2026/n	6	16.63	2018/k	11	12.36	1999/k	7.5	16.69
F30989/a	20.5	13.80	2018/n	5.5	12.95	1999/n	1.75	15.33
F30989/d	14.75	16.65	F23851/b	24.25	10.65	2008/e	21.5	10.64
F30989/g	9	18.38	F23851/e	18.5	12.83	2008/h	15.75	12.28
F30989/j	4	19.04	F23851/h	12.5	12.70	2008/k	10	13.19
F30988/a	29.5	16.55	F23851/k	6.5	13.29	2008/m	6.25	12.35
F30988/d	21.5	15.71	F23851/n	1	11.43	2008/p	0.5	11.91
F30988/g	15.25	15.04	F23852/b	23	15.93	2004/b	32	13.02
F30988/j	9.5	13.27	F23852/e	17	16.41	2004/e	26	12.62
2000/b	32.25	12.29	F23852/h	11	15.38	2004/h	20	14.83
2000/e	26	11.65	F23852/k	5	15.09	2004/k	14	14.59
2000/h	21	12.40	2003/a	27.5	15.96	2004/n	8.5	14.50
2000/k	14.75	13.13	2003/d	21.75	15.65	2004/q	2	13.23
2000/n	8.5	14.32	2003/j	10.5	14.57			
2000/q	1.75	15.31	2003/m	5	15.32			
Quartz Basin Formation: ~15 Myr ago								
F19695/a	37.75	13.53	F19698/e	9	17.46			
F19695/d	31.25	12.19	F19698/h	14.75	16.45			
F19695/g	25.5	14.54	F19698/k	21	15.24			
F19695/j	19.5	15.65	F19698/n	27.25	14.58			
F19695/m	13	15.48	F19698/q	33.5	14.82			
F19695/p	7	12.48						
F19695/s	1	12.69						
Juntura Formation: ~11 Myr ago								
F10937/a	37.5	16.77	F10936/o	9.5	14.19	F5567/h	10	15.32
F10937/d	31.5	17.78	F10936/r	5	10.54	F5567/k	4	13.43
F10937/g	25.5	17.31	F5792/f	29.5	15.10	F5568/d	35	17.73
F10937/m	14	15.76	F5792/i	23.5	13.22	F5568/g	29	18.63
F10937/p	8	13.95	F5792/l	17.5	12.02	F5568/j	23	17.35
F10936/b′	39	10.22	F5792/o	11.5	12.38	F5568/m	17	15.33
F10936/c	32	13.77	F5792/r	5	14.26	F5568/p	11	14.97
F10936/f	24.5	15.05	F5567/b	21.75	11.09	F5568/s	5	13.37
F10936/l	15.5	15.26	F5567/e	16	12.41			
Rattlesnake Formation: ~7.2 Myr ago								
F188/u	6.5	17.64	2454/k	26	14.09	F30994/g	21	14.84
F188/r	12.5	15.13	2454/n	20.5	13.90	F30994/j	27	15.38
F188/n	20	14.65	2454/t	8.25	14.81	F30994/m	33	17.50
F188/k	25.5	12.85	2070/b	42.25	12.47	F30994/p	38.5	16.27
F188/h	34.5	14.18	2070/e	36.5	13.99	F30994/s	46.5	16.40
F188/e	39	13.67	2070/h	30.75	15.16	2068/b	39	14.00
2067/b	41.75	13.81	2070/k	25	17.30	2068/e	33.5	16.95
2067/e	35.5	15.35	2070/n	19	16.36	2068/h	27.75	14.36

Table 1 (*Continued*).

Sample[a]	Distance[b]	$\delta^{18}O$	Sample[a]	Distance[b]	$\delta^{18}O$	Sample[a]	Distance[b]	$\delta^{18}O$
2067/h	29.5	15.16	2070/q	13	15.68	2068/k	22	13.00
2067/k	23.75	14.50	2070/t	4	14.18	2068/n	16	13.35
2067/n	18	12.95	2076/a	34	15.26	2068/q	10.25	14.55
2067/q	12.25	11.51	2076/d	28	15.09	2068/t	4.75	16.21
2067/t	6.75	13.72	2076/g	22.5	15.54	2565/b	32.25	13.40
2454/b	44	12.98	2076/j	16.5	16.83	2565/e	26	13.15
2454/e	38	14.07	2076/m	10.5	16.13	2565/h	21	14.80
2454/h	32	15.83	2076/p	5	18.37	2565/k	15	17.53
Glenns Ferry Formation: ~3.2 Myr ago								
F1600/b′	72	11.41	F1600/v	21.5	11.61	HAFO2213/t	56	12.12
F1600/a	68	12.22	F1600/y	15	11.81	HAFO2213/cc	39	12.46
F1600/d	59	13.13	F1600/bb	9	11.74	HAFO2213/ff	32.5	12.17
F1600/g	53.5	12.61	F1600/ee	2	13.42	HAFO2213/ii	26	11.94
F1600/j	47.5	12.84	HAFO2213/b	91	9.75	HAFO2213/ll	20.5	11.96
F1600/m	41.5	11.56	HAFO2213/e	85	11.99	HAFO2213/oo	14	11.25
F1600/p	35.5	10.51	HAFO2213/h	79.5	12.31	HAFO2213/rr	8.5	12.39
F1600/s	28	11.41	HAFO2213/q	62	12.50	HAFO2213/uu	3	13.15
Modern samples								
Cow M3/b	3	10.29	Cow P4		8.22	DH M1/z	40.5	11.51
Cow M3/e	9	10.23	Cow M2/b	31.5	12.06	DH M1/w	36	11.34
Cow M3/h	15	11.19	Cow M2/e	25.5	12.64	DH M1/t	31	10.64
Cow M3/l	22.5	11.68	Cow M2/h	20	11.89	DH M1/q	26	12.41
Cow M1/b	25	13.97	Cow M2/j	16	11.82	DH M1/n	21.5	12.97
Cow M1/e	19	14.58	Cow M2/m	10	11.18	DH M1/k	16.5	13.45
Cow M1/h	13.5	14.89	Cow M2/p	4.5	10.67	DH M1/h	11.5	14.38
Cow M1/k	7.5	15.94	DH M1/ll	60	13.15	DH M1/e	7	16.14
Cow M1/n	2	15.08	DH M1/ii	55	13.01	DH M1/b	2	16.43
Cow P3/s	3	7.31	DH M1/ff	50	10.87			
Cow P3/r	5	7.24	DH M1/cc	45.5	11.40			

[a] The identification preceding the '/' refers to the Museum sample number. Fxxxx samples were contributed by the Condon Museum at the University of Oregon; xxxx and xxxx-y samples were contributed by John Day Fossil Beds, and are catalogued as JODA xxxx; HAFO2213 was contributed by Hagerman Fossil Beds. Some JODA samples contained several teeth (e.g. in a single jaw); the number after the '-' refers to each tooth from that sample that was analyzed. Lower case letter after the '/' refers to the subsample from an individual tooth. Modern samples were not curated, so their sample IDs do not correspond to any museum.

[b] Distances are in mm from the occlusal surface (wear surface) of the tooth, rounded to the nearest 0.25 mm for fossil samples, and 0.5 mm for modern samples.

4. Results

All data reveal quasi-sinusoidal variations within and among the teeth, which we interpret as reflecting isotope seasonality (Fig. 4). The wavelength of these oscillations is 50–60 mm, implying that the vertical growth rate was ~1 mm/6–7 days and that each analysis averages 1 month's time or less. From these data we can readily obtain an estimate of the yearly range of isotope compositions (Fig. 5). The best measure of average climate for the year is arguable, but choosing range midpoints, means, or medians does not affect our interpretations. Isotope compositions and yearly seasonality have changed dramatically through time (Fig. 5). Midpoint and mean compositions decreased by ~5‰ over the last 27 million years, essentially in two periods: between 27 and 15.4 (~2‰), and between 7.2 and 0 Ma (~3‰). If the modern-day M1 teeth are disregarded, the total change increases to ~6‰. In the intervening mid- to late-Miocene, tooth $\delta^{18}O$ either stabilized, or increased slightly.

The similarity of oxygen isotope compositions

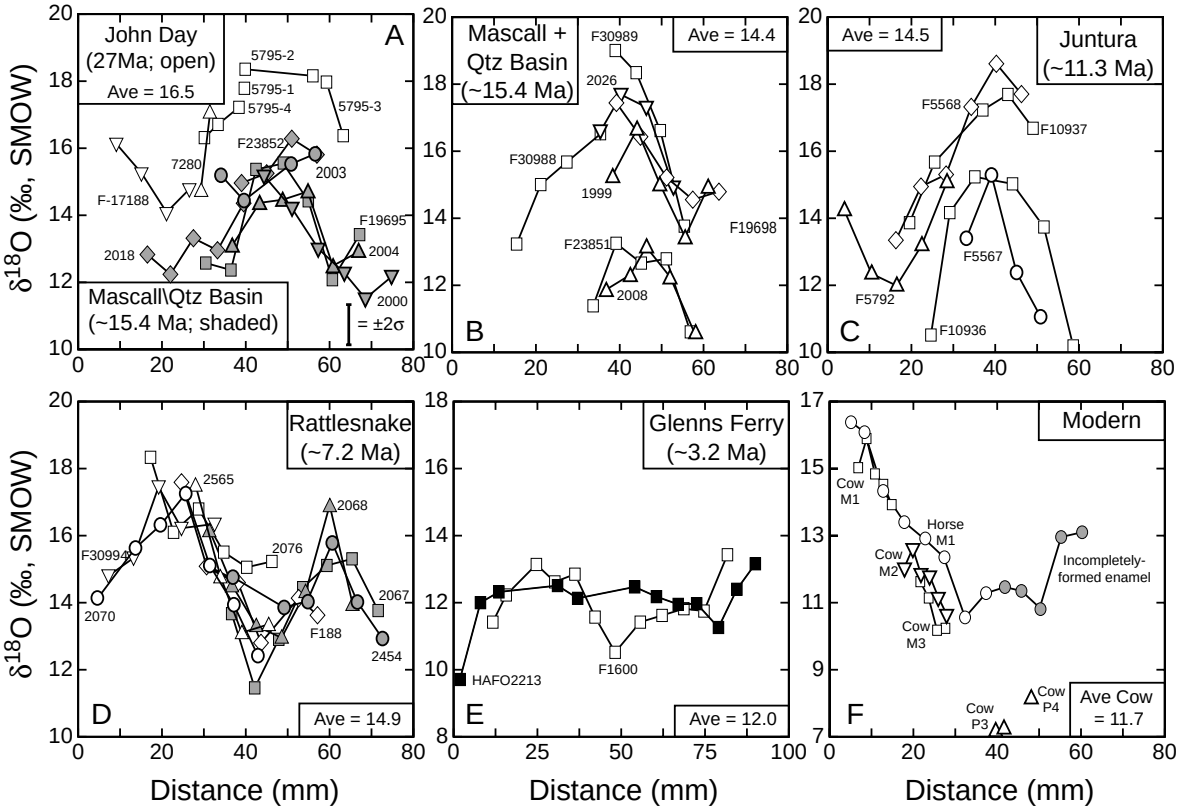

Fig. 4. Plots of 'seasonally adjusted' data for different time periods. (A) John Day and Mascall Formations, (B) Mascall and Quartz Basin Formations, (C) Juntura Formation, (D) Rattlesnake Formation, (E) Glenns Ferry Formation, (F) modern. Quasi-sinusoidal variations in isotope compositions are expected for preservation of isotope seasonality. Mascall and Quartz Basin samples exhibit both high and low amplitude signals, implying variation in seasonality that is likely related to smaller-scale fluctuations in climate. Similarity of compositions despite different localities implies general geographic independence of results. Glenns Ferry data show markedly less isotopic variability than other times. Note scale changes in panels E and F.

from different taxa at Mascall/Quartz Basin and Juntura implies either (a) no resolvable taxon-dependent differences, or (b) taxon-dependent differences counteract a climatic trend. If the latter interpretation is correct, then insofar as $\delta^{18}O$ was decreasing through time, assuming taxon-independent isotope compositions would likely underestimate the total isotopic shift. Evaluation of this possibility would require analysis of other taxa present at both Mascall/Quartz Basin and Juntura.

Large changes in isotope ranges are also apparent, with $\geq 7‰$ seasonal variability in the mid-Miocene, decreasing to only $\sim 3‰$ in the two mid-Pliocene teeth, followed by expansion to 6–8‰ in the modern samples. Mascall and Quartz Basin samples show variable zoning patterns: some samples exhibit lower $\delta^{18}O$ and reduced variability, whereas others exhibit higher $\delta^{18}O$ and increased variability. Although these variations likely reflect changes in seasonality during deposition of these rocks, the dependence of zoning pattern on stratigraphic location or type of paleosol is as yet unknown.

The magnitude of the median isotope shift and isotope seasonality must in part depend on numbers of samples. Although our data set is large by many fossil tooth standards, there are few sam-

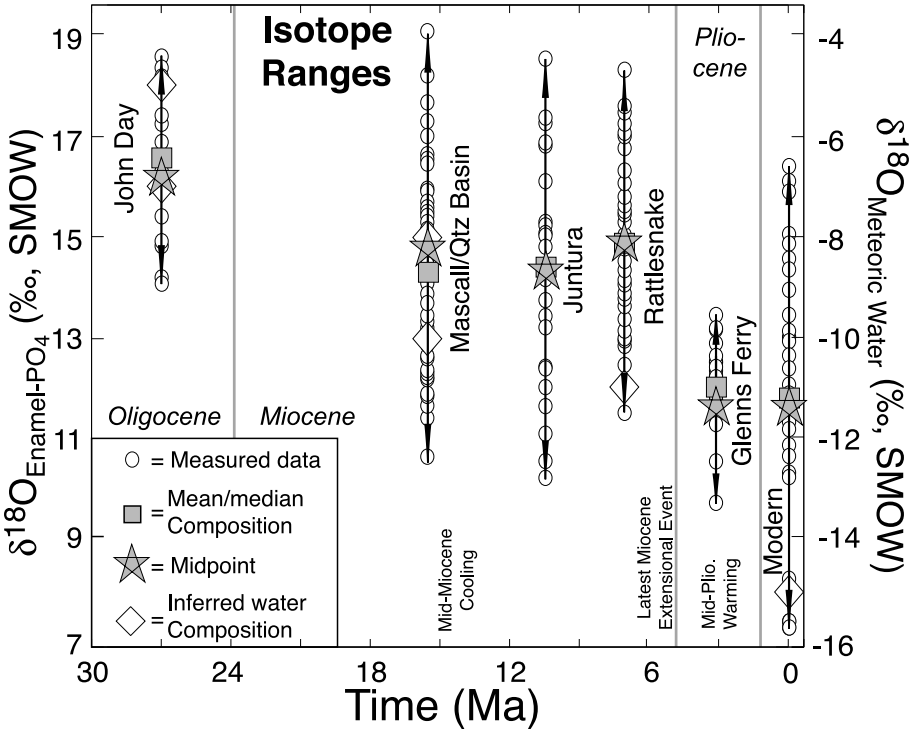

Fig. 5. Summary of isotope ranges and values through time. Vertical gray lines separate geologic epochs; double-arrowed lines are total ranges. Median and mean compositions are indistinguishable. Data outline general decrease in median and midpoint $\delta^{18}O$ through time, reflecting topographic uplift of Cascades. Period of nearly invariant $\delta^{18}O$ values between ~15.4 and ~7.2 Ma overlaps a period of reduced arc magmatism. Note that inferred change in meteoric water compositions includes both climatically and topographically driven changes.

ples in some time slices. We are confident of a major decrease in tooth $\delta^{18}O$ through time, especially in comparing Miocene vs. more recent teeth, but our interpretations do assume that the teeth we analyzed are truly representative.

5. Discussion

5.1. Global climate vs. local topographic uplift

Surprisingly, the data provide little direct evidence for a global climate signal. To a first order, global cooling would be expected to decrease $\delta^{18}O$ values of rainwater and teeth, as isotope compositions of water along coastal North America are dependent on latitude and temperature (e.g. see [4]). Warming would have the opposite effect. A rough calculation of the isotopic effects of these climatic changes can be made for source (coastal) water and hence tooth enamel (Table 2), based on: (a) estimates of secular changes to the $\delta^{18}O$ value of seawater, which has increased by about 1–1.5‰ since the mid-Miocene thermal maximum [28]; (b) the dependency of precipitation $\delta^{18}O$ values on mean annual temperature (MAT; [31–35]); and (c) the dependency of tooth enamel $\delta^{18}O$ values on rainwater composition. By focusing on source water compositions, the maximum decrease to tooth enamel $\delta^{18}O$ is calculated, because the observed decrease in the humidity of interior Oregon since the Oligocene and mid-Miocene would tend to increase tooth $\delta^{18}O$. This global climate-induced shift can then be subtracted from the main isotope trend, and the residual examined for a humidity and/or topographic signal.

The main ambiguity in predictive calculations

Table 2
Predicted isotope compositions of paleo-rainwater and -tooth enamel due to global climate change

Time (Ma)	ΔMAT (°C)	$\Delta\delta^{18}O^{RW}_{MAT}$ (‰)	$\delta\Delta^{18}O^{RW}_{IV}$ (‰)	$\delta\Delta^{18}O_{TE}$ (‰)
15.4	+3	+1.05	−0.5	+0.4
11	+1	+0.35	−0.2	+0.1
7.2	0	0.0	0.0	0.0
3.2	−2	−0.7	+0.2	−0.4
0	−5	−1.75	+0.5	−1.0

Changes in temperature and composition are relative to conditions at 27 Ma. $\Delta\delta^{18}O^{RW}_{MAT}$ and $\Delta\delta^{18}O^{RW}_{IV}$ refer to the change in rainwater composition due to a change in mean annual temperature and ice volume, respectively. If a larger ice volume effect is assumed, predicted changes to tooth composition would be less. Whereas temperature-induced changes to rainwater composition affect tooth $\delta^{18}O$ by a factor of 0.85, ice volume should affect the $\delta^{18}O$ of both seawater and atmospheric O_2 [49]. Therefore, ice volume should have a 1:1 effect on tooth enamel compositions.

is assigning a $\Delta\delta^{18}O$(precipitation)/ΔMAT value. Global geographic distributions suggest a rather strong dependence of meteoric water $\delta^{18}O$ on temperature, ~0.7‰/°C [31], whereas seasonal changes in $\delta^{18}O$ at any one mid-latitude locality show a much smaller dependence on temperature, ~0.25‰/°C [32,33]. Paleoclimate studies tend to favor the smaller dependence: the Greenland ice sheet exhibits a ~0.33‰/°C dependence [34] over a hundred thousand year time span, and tooth enamel composition changes in interior North America across the (ice-free) Paleocene–Eocene thermal maximum (ΔT ~6–8°C; [18]) imply a ~2‰ shift to rainwater compositions, or ≤ ~0.33‰/°C. Modern isotope studies of precipitation and cellulose in the Pacific Northwest suggest a dependence of ~0.4‰/°C [35]. For our calculations, we assumed a dependence of 0.35‰/°C, intermediate between estimates based on paleoclimates in other localities vs. modern climate in the study region.

Changes to MAT can be bracketed via different sources. Detailed paleoclimate studies [36] indicate temperatures were ~4°C higher at the mid-Pliocene thermal maximum, and paleosol studies suggest MAT was 3–6°C warmer in the mid-Oligocene [8]. Many leaf margin interpretations are compromised by age ambiguities or inconsistencies among sites, but two mid-Miocene (~13 Ma) localities both indicate a 4–5°C higher MAT [37]. These sources imply that the mid-Miocene thermal maximum (~15 Ma) must have been at least 6°C warmer than at present. Alternatively, comparing the shift in global foraminifera $\delta^{18}O$ curve [28] with modern vs. Pliocene climates implies that for northern mid-latitudes, eastern Pacific, $\Delta T/\Delta\delta^{18}O$(marine foraminifera) was ~4°C/‰. Extrapolation of this dependence using the foraminiferal isotope curve probably overestimates temperature changes, but implies the Miocene and Oligocene of central Oregon were about 11 and 7°C warmer, respectively, than today. From all observations, we assume a MAT ~8°C higher at the Miocene thermal maximum, and ~5°C higher in the late Oligocene compared to today, with other temperatures scaled accordingly via the foraminiferal isotope curve.

The predicted curve of isotope differences relative to the Oligocene samples (Fig. 6; Table 2) corresponds to the expected isotopic effects on tooth enamel $\delta^{18}O$ values due to changes in source water composition alone. There is little change predicted because, whereas cooling will decrease meteoric water $\delta^{18}O$, concomitant growth of ice sheets will increase seawater (source) $\delta^{18}O$. In fact, if decreasing local humidity since the mid-Miocene were considered, then predicted tooth $\delta^{18}O$ would show a net increase. Most importantly, the effects of global climate change imply an isotopic pattern and magnitude markedly unlike the observed trends. In general, the expected shift to tooth enamel $\delta^{18}O$ due to global cooling is only ~1‰, whereas the observed shift is nearly 5‰ (if modern M1 analyses are included; ~6‰ excluding them). The details of the observed vs. predicted trends also show disparities. Global warming from the Oligocene to the mid-Miocene (27–15.4 Ma) should have caused an increase in tooth $\delta^{18}O$ values, whereas a decrease is observed, and global cooling in the mid-Miocene (15.4–11 Ma) should have caused a small decrease in tooth $\delta^{18}O$ values, whereas no change or a slight increase occurred. Identification of climatic effects since the Pliocene is compromised because of temporal uncertainties in placing

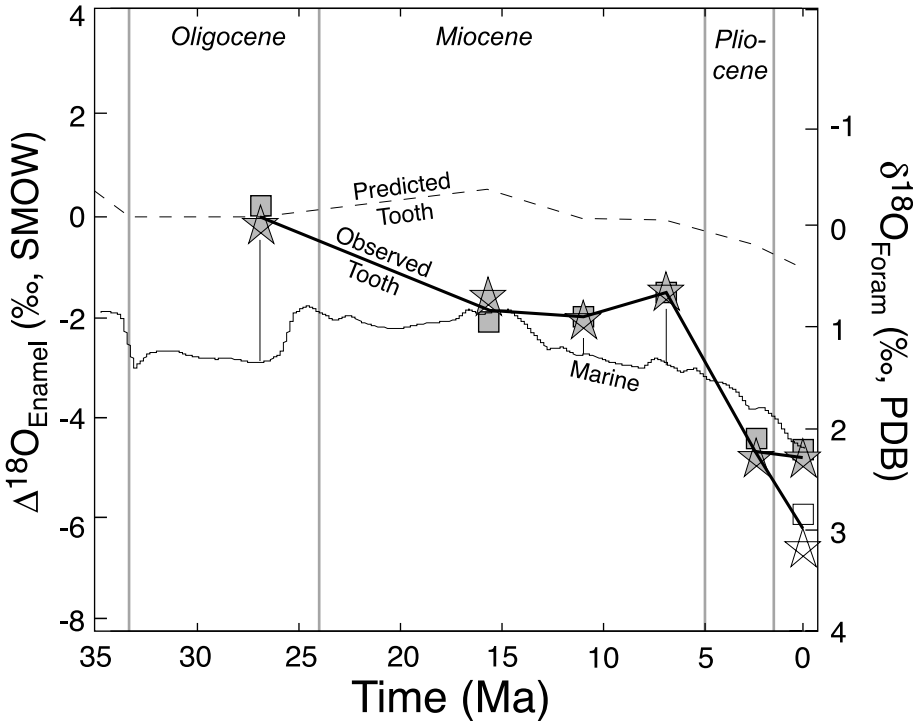

Fig. 6. Comparison of changes in $\delta^{18}O$ values of fossil teeth (symbols and thick solid line) with the benthic foraminiferal isotope record [28] (thin solid line), and with semi-quantitative predictions for tooth compositions assuming only globally driven changes to source water isotopic compositions (dashed line). Tooth compositions are plotted relative to John Day samples. Extension of dashed line prior to 27 Ma is schematic and based on marine foraminifera record. The scale for the marine record has been reversed to illustrate better that lower $\delta^{18}O_{Foram}$ values correspond to higher temperatures and lower ice volume than higher values (i.e. T increases upward). In general, higher predicted values for tooth $\delta^{18}O$ correspond to higher T and/or lower humidity. Open symbols are compositions of modern samples, omitting M1 analyses. Thin vertical lines highlight particular discrepancies between the terrestrial and marine isotope records: large climatic and isotopic shifts evident in the marine record are not reflected in the isotope systematics of the fossil teeth. The expected climatic effects on tooth $\delta^{18}O$ are much smaller than the observed changes, likely implying the dominance of regional topography and tectonics.

the Glenns Ferry samples precisely into the Pliocene climatic record, plus uncertainties in whether to include M1 teeth in our modern sample set. A trend towards lower $\delta^{18}O$ would be consistent with global cooling since the mid-Pliocene thermal maximum, and thus the latest part of the isotope record, likely embeds an important climatic signal.

The disparity between our $\delta^{18}O$ record and expectations of global climate change does not imply that global climate change had no effects in central Oregon. As discussed by Retallack et al. [8] and Bestland et al. [38], there are strong correlations in central Oregon between secular changes in paleosol type and global climate. However, paleosols and tooth enamel do not encode the same climatic signals. Paleosols are most strongly influenced by yearly precipitation, precipitation seasonality, and average humidity, whereas tooth $\delta^{18}O$ is most strongly influenced by rainwater $\delta^{18}O$ values, with humidity as a secondary effect. If global climate change affected yearly precipitation and humidity, but not rainwater $\delta^{18}O$, then paleosols might change dramatically, where tooth enamel did not. However, this implies that some other climatic agent is responsible for changes in rainwater $\delta^{18}O$ in central Oregon.

Overall the systematic decrease in equid $\delta^{18}O$ compositions since the Oligocene must primarily have resulted from topographic uplift. The rise of

the Cascades increased the degree of rainout, progressively lowering the $\delta^{18}O$ of rainwater in central Oregon through time. If $\sim 1‰$ of the 4.7‰ decrease in tooth $\delta^{18}O$ values is explainable from climate change, then the residual 3.7‰ isotope effect must be due to topographic uplift. Although a 3.5–4‰ isotope shift is smaller than the modern-day isotopic difference in rainwater across the range ($\sim 7‰$), the dependence of biogenic phosphate $\delta^{18}O$ on water $\delta^{18}O$ is not 1:1, and humidity also plays an important role in controlling phosphate $\delta^{18}O$. For a 3.7‰ shift in tooth $\delta^{18}O$ composition, global correlations and theoretical models [15,21] both imply a $\sim 4.5‰$ change in meteoric water $\delta^{18}O$ value. This assumes that animals all drink from surface water sources, and that surface water is a 1:1 monitor of meteoric water. However, lower humidity promotes increased evaporation that will enrich surface water and food sources in $\delta^{18}O$. Because relative humidity decreased by $\geq 15\%$ since 27 Ma, this effect must also be considered and subtracted. Theoretical and natural studies [14,15] suggest that a $\geq 15\%$ decrease in relative humidity acting alone should have increased tooth $\delta^{18}O$ values by $\geq 1.5–3‰$. Thus, for a residual change in tooth $\delta^{18}O$ values of 3.7‰, we estimate the change in rainwater $\delta^{18}O$ in the interior due to topographic uplift was $\geq 6–8‰$, similar to the modern-day effect across the range. That is, our data are most consistent with a monotonic increase in Cascade range height between 27 Ma and today, in support of one model [10]. Within the limits of our current data set, there could have been pulsed uplift. For example, there could have been little change in range height between 15.4 and 7.2 Ma, depending on assumed humidity changes. This issue could potentially be resolved via analysis of other taxa from the mid- to late Miocene (7–16 Ma). Regardless, our data do not support sudden uplift to modern heights any time in the past or major uplift in the mid-Miocene. This conclusion is inconsistent with most previous topographic models [12,13].

5.2. Topographic uplift mechanisms

Prolonged uplift of the Cascades rules out catastrophic forcing mechanisms, including lithospheric delamination [39], which operates too quickly (several million years) [40] to explain our data. Instead, a quasi-continuous process is required. Continuous fluxing of the mantle wedge and melt extraction above the subducting Juan de Fuca plate would progressively increase buoyancy by stripping out dense Fe- and Al-rich silicates and oxides from the mantle and transforming them into less dense mid/upper crustal materials. However, the mantle wedge above subduction zones likely undergoes forced convection, replacing old, more buoyant mantle with new dense mantle [41]. Also, there is no evidence for systematic major changes in melt type or temperature, as is expected from melting a progressively more refractory source. Instead, we believe magmatic style and location principally affected range height – the longer the arc was active, the thicker and higher it became. This model accords well with simple isostatic models because the crust under the Cascades is thicker than average [42], and the additional thickness translates into a mean range height of ~ 1500 m, similar to observed elevations. Furthermore, the one isotopically stable time (15.4–7.2 Ma) is when the Columbia River Basalt magmatism was most active, and the arc was relatively quiescent.

This model implies that former long-lived continental arcs, such as the Sierra Nevada and Gangdese (trans-Himalayan) batholiths, must have been climatically important topographic barriers by the end of magmatism. Insofar as climatic stress may drive evolution, such arcs may additionally influence species richness and evolutionary radiations. Although a link between *global* climate change and biotic events has recently been criticized [43], in our view *regional* climate is a more effective evolutionary agent. For Oregon, equid evolution has been linked to the rise and evolution of grasslands [44], and possibly increasing Cascade topography drove climatic stresses (aridity and perhaps precipitation variability) with strong herb and herbivore selective pressure. This in turn would have affected both grasslands and their grazers, possibly promoting the dramatic mid-Miocene radiation of equids.

5.3. Seasonality changes

Although we have analyzed only two teeth from the mid-Pliocene, in comparison with composite data from other time intervals they both exhibit reduced isotope seasonality, as also indicated by other isotope, paleofaunal, and paleofloral studies in Idaho for the Pliocene [45,46]. For example, assuming a 0.35‰/°C dependence of meteoric water composition on temperature, and accounting for factors of 0.85 both for reservoir effects in animals and for the correlation between biogenic and meteoric water $\delta^{18}O$, the 6‰ seasonality exhibited by some Miocene teeth could reflect a mean annual range in temperature (MART) approaching 25°C. In contrast, the 3‰ seasonality indicated by the Pliocene teeth suggests MART ~12°C. One possible explanation for reduced seasonality invokes global warming during the Pliocene thermal maximum. Clearly the Earth was at least as warm or warmer between 27 and 7 Ma compared to the Pliocene. However, this warmth occurred within the context of radically different boundary conditions. For example, the Tibetan plateau may not have achieved maximal climatic effect until ~3.5 Ma [47], and full closure of the Isthmus of Panama and consequent reorganization of ocean circulation patterns did not occur until 3.5–4 Ma [48]. Because of these different globally important factors, a small increase in temperature in the mid-Pliocene may have affected seasonality in the western interior of the US quite differently than previous warm periods.

Alternatively, climate and/or water compositions may have been buffered by a large lake (Lake Idaho) that was present sporadically in Idaho during the Pliocene. Large bodies of water average seasonal extremes much more effectively than small streams or soil water, and so exhibit less isotope variability. If equids obtained most of their water and food near the lake, then they would record a damped isotopic variability, and so not record full MART in comparison to times when the lake was not present or was smaller. This hypothesis can be tested by determining isotope zoning in teeth from times when the lake was large vs. when it was small.

Acknowledgements

Funded by NSF Grant EAR9909568 and a grant from the University of South Carolina Research and Productive Scholarship Fund. We thank W. Orr and N. Farmer for providing samples from collections at the University of Oregon and Hagerman Fossil Beds, and S. Foss, D. Findeisen, A. Pajak, L.R. Rogers, M. Smith, and L. Vella for help in the field. J. Quade and H. Fricke provided excellent and constructive reviews.

References

[1] M.E. Raymo, W.F. Ruddiman, Tectonic forcing of late Cenozoic climate, Nature 359 (1992) 117–122.
[2] P. England, P. Molnar, Surface uplift, uplift of rocks, and exhumation of rocks, Geology 18 (1990) 1173–1177.
[3] Western Regional Climate Center, http://www.wrcc.dri.edu.
[4] T.B. Coplen, C. Kendall, Stable hydrogen and oxygen isotope ratios for selected sites of the U.S. Geological Survey's NASQAN and Benchmark Surface-water Networks, in: USGS Open-File Report, U.S. Geological Survey, 2000.
[5] E.A. Sammel, R.W. Craig, The geothermal hydrology of Warner Valley, Oregon: A reconnaissance study, U.S. Geological Survey Professional Paper 1044-I, 1981.
[6] S.E. Ingebritsen, R.H. Mariner, D.E. Cassidy, L.D. Shepherd, T.S. Presser, M.K.W. Pringle, L.D. White, Heatflow and water-chemistry data from the Cascade Range and adjacent areas in North-Central Oregon, U.S. Geological Survey Open-File Report 88-702, 1988.
[7] M. Ashwill, Seven fossil floras in the rain shadow of the Cascade Mountains, Oregon, OR Geol. 45 (1983) 107–111.
[8] G.J. Retallack, E.A. Bestland, T.J. Fremd, Eocene and Oligocene paleosols of central Oregon, Geological Society of America Special Paper 344, 2000.
[9] National Climatic Data Center, http://lwf.ncdc.noaa.gov.
[10] P.E. Hammond, A tectonic model for evolution of the Cascade Range, Society of Economic Paleontologists and Mineralogists Special Publication 3 (1979) 219–238.
[11] G.A. Smith, L.W. Snee, E.M. Taylor, Stratigraphic, sedimentologic, and petrologic record of late Miocene subsidence of the central Oregon High Cascades, Geology 15 (1987) 389–392.
[12] G.R. Priest, Volcanic and tectonic evolution of the Cascade volcanic arc, central Oregon, J. Geophys. Res. 95 (1990) 19583–19599.
[13] D.R. Sherrod, Geology, petrology, and volcanic history of a portion of the Cascade range between latitudes 43°-44° north central Oregon, USA, Ph.D., University of California, Santa Barbara, 1986.

[14] B. Luz, A.B. Cormie, H.P. Schwarcz, Oxygen isotope variations in phosphate of deer bones, Geochim. Cosmochim. Acta 54 (1990) 1723–1728.
[15] M.J. Kohn, Predicting animal $\delta^{18}O$: Accounting for diet and physiological adaptation, Geochim. Cosmochim. Acta 60 (1996) 4811–4829.
[16] H.C. Fricke, J.R. O'Neil, Inter- and intra-tooth variation in the oxygen isotope composition of mammalian tooth enamel phosphate; implications for palaeoclimatological and palaeobiological research, Palaeogeogr. Palaeoclimatol. Palaeoecol. 126 (1996) 91–99.
[17] M.J. Kohn, M.J. Schoeninger, J.W. Valley, Variability in herbivore tooth oxygen isotope compositions: reflections of seasonality or developmental physiology?, Chem. Geol. 152 (1998) 97–112.
[18] H.C. Fricke, W.C. Clyde, J.R. O'Neil, Intra-tooth variations in $\delta^{18}O(PO_4)$ of mammalian tooth enamel as a record of seasonal variations in continental climate variables, Geochim. Cosmochim. Acta 62 (1998) 1839–1850.
[19] L.K. Ayliffe, A.R. Chivas, M.G. Leakey, The retention of primary oxygen isotope compositions of fossil elephant skeletal phosphate, Geochim. Cosmochim. Acta 58 (1994) 5291–5298.
[20] Y. Kolodny, B. Luz, O. Navon, Oxygen isotope variations in phosphate of biogenic apatites. I. Fish bone apatite-rechecking the rules of the game, Earth Planet. Sci. Lett. 64 (1983) 398–404.
[21] M.J. Kohn, T.E. Cerling, Stable isotope compositions of biological apatite, Rev. Mineral. 49 (2002), in press.
[22] F. Albarède, Introduction to Geochemical Modeling, Cambridge University Press, Cambridge, 1995, 543 pp.
[23] J.R. O'Neil, L.J. Roe, E. Reinhard, R.E. Blake, A rapid and precise method of oxygen isotope analysis of biogenic phosphate, Isr. J. Earth Sci. 43 (1994) 203–212.
[24] D.L. Dettman, M.J. Kohn, J. Quade, F.J. Ryerson, T.P. Ojha, S. Hamidullah, Seasonal stable isotope evidence for a strong Asian monsoon throughout the past 10.7 m.y., Geology 29 (2001) 31–34.
[25] T.W. Vennemann, H.C. Fricke, R.E. Blake, J.R. O'Neil, A. Colman, Oxygen isotope analysis of phosphates: a comparison of techniques for analysis of Ag_3PO_4, Chem. Geol. (2002) 321–336.
[26] T. Fremd, E.A. Bestland, G.J. Retallack, John Day Basin Paleontology, Northwest Interpretive Association, Seattle, WA, 1997, 80 pp.
[27] W.K. Hart, M.E. Brueseke, Analysis and dating of volcanic horizons from Hagerman Fossil Beds National Monument and a revised interpretation of eastern Glenns Ferry Formation chronostratigraphy, National Park Service Report 1443-PX9608-97-003, 1999, 37 pp.
[28] J. Zachos, M. Pagani, L.C. Sloan, E. Thomas, K. Billups, Trends, rhythms and aberrations in global climate 65 Ma to present, Science 292 (2001) 686–693.
[29] K.A. Hoppe, R. Amundson, Interpreting the significance of stable isotopic variations within mammalian teeth: evaluating the influence of viological vs. environmental factors, Geological Society of America Abstracts with Program 33 (2001) A113–A114.
[30] C. Gadbury, L. Todd, A.H. Jahren, R. Amundson, Spatial and temporal variations in the isotopic composition of Bison tooth enamel from the early Holocene Hudson-Meng bone bed, Nebraska, Palaeogeogr. Palaeoclimatol. Palaeoecol. 157 (2000) 79–93.
[31] W. Dansgaard, Stable isotopes in precipitation, Tellus 16 (1964) 436–468.
[32] H.C. Fricke, J.R. O'Neil, The correlation between $^{18}O/^{16}O$ ratios of meteoric water and surface temperature its use in investigating terrestrial climate change over geologic time, Earth Planet. Sci. Lett. 170 (1999) 181–196.
[33] IAEA, Statistical treatment of data on environmental isotopes in precipitation, Technical Report No. 331, International Atomic Energy Agency, Vienna, 1992.
[34] R.B. Alley, K.M. Cuffey, Oxygen- and hydrogen-isotopic ratios of water in precipitation beyond paleothermometry, Rev. Mineral. 43 (2001) 527–553.
[35] R.L. Burk, M. Stuiver, Oxygen isotope ratios in trees reflect mean annual temperature and humidity, Science 211 (1981) 1417–1419.
[36] H.J. Dowsett, J.A. Barron, R.Z. Poore, R.S. Thompson, T.M. Cronin, S.E. Ishman, D.A. Willard, Middle Pliocene Paleoenvironmental Reconstruction: PRISM2, United States Geological Survey, 1999.
[37] J.A. Wolfe, Tertiary climatic changes at middle latitudes of western North America, Palaeogeogr. Palaeoclimatol. Palaeoecol. 108 (1994) 195–205.
[38] E.A. Bestland, G.J. Retallack, C.C. Swisher, Stepwise climate change recorded in Eocene-Oligocene paleosol sequences from central Oregon, J. Geol. 105 (1997) 153–172.
[39] P. Bird, Continental delamination and the Colorado Plateau, J. Geophys. Res. 84 (1979) 7561–7571.
[40] G.A. Houseman, D.P. McKenzie, P. Molnar, Convective instability of a thickened boundary layer and its relevance for the thermal evolution of continental convergent belts, J. Geophys. Res. 86 (1981) 6115–6132.
[41] Y. Furukawa, Magmatic processes under arcs and formation of the volcanic front, J. Geophys. Res. 93 (1993) 8309–8319.
[42] W.D. Mooney, C.S. Weaver, Regional crustal structure and tectonics of the Pacific coastal states; California, Oregon, and Washington, in: W.D. Mooney (Ed.), Geophysical framework of the continental United States, Memoir - Geological Society of America 172, Geological Society of America, 1989, pp. 129–161.
[43] J. Alroy, P.L. Koch, J.C. Zachos, Global climate change and North American mammalian evolution, Paleobiology 26 (Supplement) (2000) 259–288.
[44] G.J. Retallack, Cenozoic expansion of grasslands and climatic cooling, J. Geol. 109 (2001) 407–426.
[45] G.R. Smith, W.P. Patterson, Mio-Pliocene seasonality on the Snake River plain comparison of faunal and oxygen isotopic evidence, Palaeogeogr. Palaeoclimatol. Palaeoecol. 107 (1994) 291–302.

[46] R.S. Thompson, Pliocene and early Pleistocene environments and climates of the western Snake River Plain, Idaho, Mar. Micropaleontol. 27 (1996) 141–156.
[47] D.K. Rea, H. Snoeckx, L.H. Joseph, Late Cenozoic eolian deposition in the North Pacific: Asian drying, Tibetan uplift, and cooling of the northern hemisphere, Paleoceanography 13 (1998) 215–224.
[48] G.H. Haug, R. Tiedemann, Effect of the formation of the Isthmus of Panama on Atlantic Ocean thermohaline circulation, Nature 393 (1998) 673–676.
[49] M. Bender, L.D. Labeyrie, D. Raynaud, C. Lorius, Isotopic composition of atmospheric O_2 in ice linked with deglaciation and global primary productivity, Nature 318 (1985) 349–352.